Available online at www.ijournalse.org

Emerging Science Journal

(ISSN: 2610-9182)

Vol. 9, No. 6, December, 2025

DC Motor Angular Speed Controller Using an Embedded Microcontroller-Based PID Controller

Alfian Ma'arif [1], Ikhwan Nugraha [1], Hari Maghfiroh [2*], Furizal [3], Iswanto Suwarno [4]

[1] *Department of Electrical Engineering, Universitas Ahmad Dahlan, Yogyakarta 55191, Indonesia.*

[2] *Department of Electrical Engineering, Universitas Sebelas Maret, Surakarta 57126, Indonesia.*

[3] *Department of Research and Development, Peneliti Teknologi Teknik Indonesia, Sleman 55281, Indonesia.*

[4] *Department of Electrical Engineering, Universitas Muhammadiyah Yogyakarta, Yogyakarta 55183, Indonesia.*

Abstract

This research presents the implementation of a Proportional Integral Derivative (PID) controller to control the angular speed of a Direct Current (DC) motor using an embedded system (microcontroller). The system's hardware consists of an Arduino microcontroller, a DC motor with an encoder sensor, a driver motor, and a power supply. Proportional control regulates the response proportionally to the calculated error, while integral control manages the cumulative error over time, and derivative control responds to the rate of change of the error, preventing overshoot. With a proper combination, PID control achieves stability, speeds up response, and reduces overshoot, improving overall system performance. Based on experimental data, the DC motor angular speed control system using PID control achieves the best results, in which the parameter values are Kp=1; Ki=0.3; and Kd=0.6. The augmented system responded with 0.0890 seconds of the rise time, 11.772 seconds of settling time, and 0.12 seconds of the peak time, with an overshoot of less than 10% (7%).

Keywords:

DC Motor; PID Controller; Arduino; Speed Angular; Embedded Microcontroller.

Article History:

Received:	13	December	2024
Revised:	12	July	2025
Accepted:	23	September	2025
Published:	01	December	2025

1- Introduction

Direct Current (DC) motors are essential components in many home and industrial appliances due to their ability to convert electrical energy into mechanical motion [1]. The advantage of a DC motor is that it is easy to control and implement [2]. Therefore, DC motors have many applications [3]. It has been implemented in various applications such as magnetic stirrers [4], steering [5], mobile robots [6], wheeled robots [7], water pumps [8], Conveyor [9], inverted pendulum [10], and process control [11]. One of the important characteristics of DC motors is the ability to adjust the angular speed by regulating the applied voltage [12]. However, their natural characteristics show inefficiencies in terms of stability [13], especially when the applied voltage does not match the operational voltage [14]. This leads to an undesirable slowdown or increase in the angular speed of the motor, resulting in a decrease in energy usage efficiency [15].

Previous studies have implemented some control techniques for the angular speed of DC Motor systems, such as PID control [16], Fractional Order PID (FOPID) control [17], State Feedback [18], Linear Quadratic Regulator [19], Sliding

* **CONTACT**: hari.maghfiroh@staff.uns.ac.id

DOI: http://dx.doi.org/10.28991/ESJ-2025-09-06-03

Mode Control [20], and Fuzzy Logic Controller (FLC) [21, 22]. PID controllers have become popular in controlling the speed and response of DC motors [23-25]. Its main advantage lies in its adaptability across a wide range of operational conditions, allowing for easier practical use in both daily life and industrial applications [26, 27]. In the context of angular speed control in DC Motors, PID Controllers are a promising solution to improve the stability and response of the motor [28].

Some previous research has implemented PID controllers for DC motor systems [29-34]. However, those pieces of research were limited to simulations with ideal conditions [35, 36]. Hardware implementation of the controller is crucial since application in the real world is not ideally conducted, and disturbance exists [37]. Evaluating and examining the controller in real-time application is highly necessary to assess whether the method is suitable or not in the real condition [38].

This research aims to evaluate and apply the effectiveness of PID Controllers in regulating the angular speed of DC Motors. The method that will be used is the PID Controller applied on an Arduino-based system to regulate the angular speed of the DC Motor. Testing will involve variations in the voltage applied to the motor to observe its response to various PID settings implemented through Arduino. The benefits of this research are expected to support the theoretical understanding of automatic control on DC Electric Motors. The implementation of an effective PID Controller on a DC Motor using the Arduino platform has the potential to provide a simpler yet efficient solution for optimally regulating the speed of an electric motor. This is expected to increase operational efficiency in various industrial sectors and daily life without requiring an overly complex approach.

The paper structure is as follows. The first part is an introduction that explains the research background. The second part is the method that consists of a comprehensive review of DC motor system, Pulse Width Modulation (PWM), Proportional Integral Derivative (PID) Controller, Control System Diagram, Wiring Diagram and Flowchart Diagram. The third part is the result and discussion that consists of hardware implementation, PWM experiments and calibration encoder, Proportional (P) Controller Experiments, Proportional (PI) Controller Experiments and Proportional Integral Derivative (PID). The last part is the conclusion and future work.

2- Method

2-1- DC Motor

Direct Current (DC) Electric Motor is a device that converts electrical energy into kinetic energy or movement [39]. DC motors are also referred to as Direct Current Motors. As the name suggests, DC Motor has two terminals and requires a direct current or DC voltage to move [40]. This DC motor produces a number of revolutions per minute, commonly known as Revolutions Per Minute (RPM), and can be made to rotate clockwise or counter clockwise if the polarity of the electricity given to the DC motor is reversed [41]. DC motors are one of the main drivers that are widely used in industry today. In the past years, most of the small servo motors used for control purposes were of the Alternating Current (AC) type. In reality, AC motors are more difficult to control, especially for angular position control, and their characteristics are quite nonlinear, which makes analytical tasks more difficult [42]. AC motors are costly due to their brushes and commutators. Moreover, AC motors with changing flux are only suitable for certain control applications.

Figure 1 shows parts of the DC motor. Based on Figure 1, the important parts of DC motor are the Stator Magnets, Coils, and Commutator. A simple DC motor has two field magnets: the north poles and the south poles. Magnetic energy lines expand across the open space between the poles from north to south [43, 44]. There are one or more electromagnets for larger or more complex motors. When an electrical current enters the DC motor coil, it will become an electromagnet. DC motor coils are cylindrical and connected to the drive axle to move the load. In the case of small DC motors, the DC motor coil rotates in a magnetic field formed by the poles until the north and south poles of the magnet change location. DC motor commutators are mainly found in DC motors. Its use is to reverse the direction of electrical current in the DC motor coil, and it also helps to transmit the electrical current between the DC motor coil and the power source.

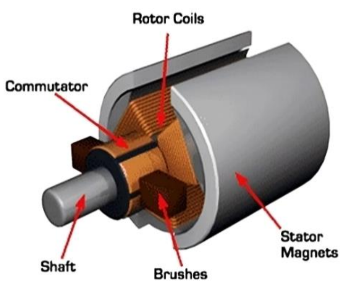

Figure 1. The parts of DC Motor

2-2- Pulse Width Modulation

Pulse Width Modulation (PWM) is a technique used to control power in electronic devices by regulating the duration of the signal pulses given to the device [45, 46]. In the context of this research, PWM is used to control the signal pulse on a DC motor and adjust its angular speed as needed [47]. The basic principle of PWM lies in modulating the duty cycle of a digital signal; the duty cycle is known as the ratio of a period when the signal is in the ON state (ON time) compared to the total period of its cycle (ON+OFF time) [48]. The illustration of the PWM output signal shows a signal wave with a consistent period, but the pulse width in the active (on) phase can be changed as needed. Figure 2 illustrates a visualization of the PWM signal output.

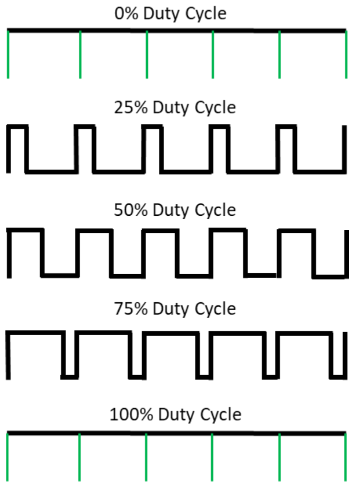

Figure 2. PWM Signal illustration

Figure 2 displays 5 examples of PWM signal output with different duty cycles with a source voltage of 5 V, ranging from 0% to 100%. When the duty cycle reaches 0%, there is no signal pulse in the active condition, making the output voltage 0 V. However, if the duty cycle given is 50%, the working voltage released from PWM is 2.5 V, obtained based on the PWM formula in Equation 1.

$$V_{PWM} = (Pulse_{on})/(Pulse_{on} + Pulse_{off}) \times V_{supply} \quad (1)$$

Equation 1 describes the relationship between the PWM output voltage (V_{PWM}) and the ratio of the active pulse time ($Pulse_{on}$) to the total cycle period ($Pulse_{on} + Pulse_{off}$), multiplied by the source voltage (V_{source}). This formula allows the calculation of the output voltage based on the duration of its ON and OFF state in one PWM cycle [49].

2-3- Proportional Integral Derivative (PID) Controller

Proportional, Integral, and Derivative (PID) control is a significant control method in engineering [50]. It utilizes feedback from the controlled system to ensure precision and stability in its operation. Consisting of three main parameters, namely Proportional (P), Integral (I), and Derivative (D) control [51], PID is used in various fields such as process control [52, 53], robotics [54, 55], power systems [56], and others [57]. The use of the PID method on a system can be customized depending on the desired response and characteristics of the system being controlled [58]. This arrangement allows controls that rely solely on proportional (P), a combination of proportional and integral (PI) [59], or use proportional, integral, and derivative simultaneously (PID), to produce the desired response to a plant.

The role of each PID component is vital in the control process [60]. Proportional control responds directly to the error between the setpoint and the system output. Integral handles errors that accumulate over time, generating correction signals for errors that persist over long periods. Meanwhile, derivative control responds to the rate of change in the error [61]. These three components work together to improve system response, reduce error, and increase stability, thereby achieving the desired setpoint. Equation 2 displays the mathematical form of the PID equation [62].

$$u(t) = K_p e(t) + K_i \int_0^t e(t)dt + K_d \frac{de(t)}{dt} \quad (2)$$

In application, PID has several basic terminology that is important to understand. Common concepts include setpoint (the expected value of the system), control signal with the symbol of $u(t)$, output with the symbol $y(t)$ (the actual value of the system), and error with the symbol $e(t)$ (the difference between setpoint and output) [63]. The PID controller then uses the calculated error to calculate the correction signal required to achieve the desired value [64]. Understanding these basic concepts is important to effectively utilizing PID control in various application situations.

2-4- Control System Diagram

The design of the control system begins with the first step of creating an overall control system diagram. The diagram serves as a visual representation of the relationship between the main components of the augmented system. At the initial stage, the identification of key elements such as the DC motor, PID control, speed sensor in the form of an encoder, and speed setpoint form the basis of the diagram. Figure 3 facilitates a clear understanding of the interactions between elements, depicting the flow of signals or information in the augmented control system.

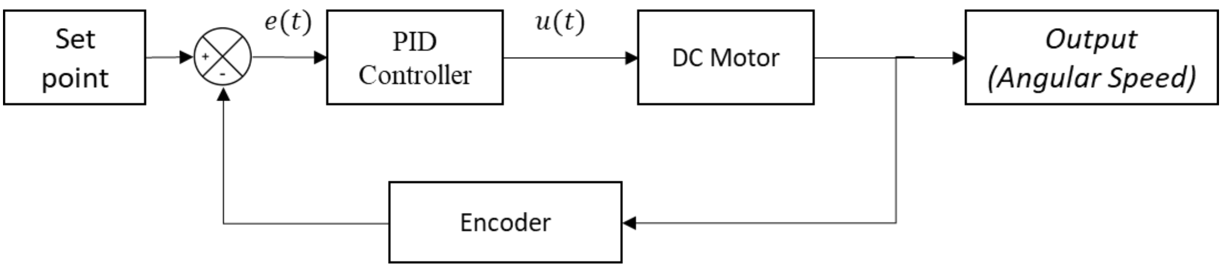

Figure 3. Control System Diagram

Based on Figure 3, the first step is to set the speed setpoint as the initial input. The setpoint signal is then compared with the encoder feedback to generate the error, which is the difference between the desired and actual values. The generated error becomes the input for the PID control, which then generates a control signal to regulate the DC motor. The DC motor responds by generating an angular speed corresponding to the received control signal. The encoder measures the actual speed of the motor, providing feedback to the system. The entire process is repeated continuously, with the PID control adjusting the output signal to minimize the error and achieve the desired speed setpoint.

2-5- Wiring Diagram

The design of the wiring diagram used to control the DC motor and the system to be developed requires a voltage input of 12VDC (9V battery) and a setpoint input from a potentiometer. The wiring diagram is designed using the Fritzing software and organized to provide a more detailed picture related to the connection configuration and the role of each component in the system.

For a more detailed understanding of the connection diagram in Figure 4, a detailed explanation is provided in Table 1. The table shows the configuration of the Arduino interface, motor driver, DC motor, encoder sensor, potentiometer, and power source. The purpose of this explanation is to provide a more detailed picture of the relationship settings between these components in the system.

Table 1. Wiring Connection

Arduino UNO	Motor Driver LN298	Motor DC	Potentiometer
3V3	-	3.3V	-
GND	GND	GND	GND
5V	5V	-	5V
V_{IN}	12V	-	-
3	IN1	-	-
4	IN2	-	-
5	ENA	-	-
6	-	C2	-
7	-	C1	-
A0	-	-	Data
-	Out1	M1	-
-	Out2	M2	-

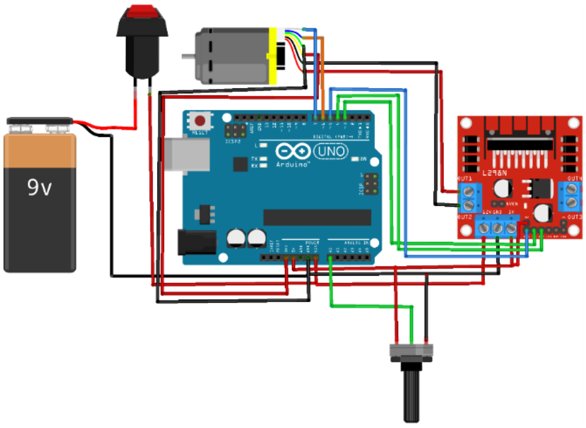

Figure 4. Wiring Diagram

2-6- Flowchart Diagram

A system flowchart is a visual representation that describes the relationship of system steps (processes). In the context of this research, the system flow chart will be used to explain in detail how the system works, starting from initialization to setting the watering interval based on temperature and humidity data. Figure 5 shows the system flow chart that provides a visual representation of the steps executed by the system.

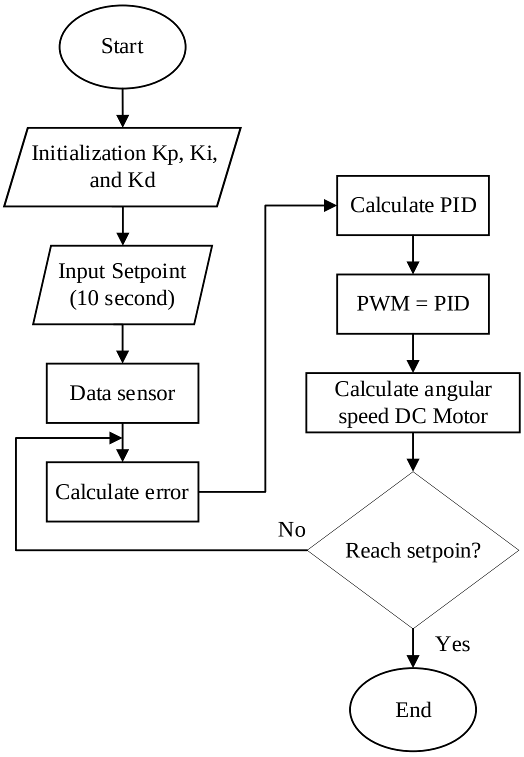

Figure 5. Flowchart Diagram

Based on the flow chart in Figure 5, the initial stages of the system begin with the initialization of the Kp, Ki, and Kd parameters. Next, the setpoint input is controlled using a potentiometer for a period of 10 seconds. The next process involves measuring the encoder sensor data to generate information about Rotations Per Minute (RPM). The data measured by the sensor is then used to calculate the error, which is further used in the Proportional-Integral-Derivative (PID) calculation. The results of the PID calculation are integrated as PWM input to the motor driver. The speed of the DC motor is measured and maintained until it reaches the desired setpoint. If the desired setpoint has not been reached, the process is repeated by recalculating the error; if the setpoint has been reached, the system runs the motor optimally.

3- Results and Discussion

3-1- Hardware Implementation

In this sub-chapter, we explain the hardware implementation used in this research. The hardware implementation is divided into two main parts: internal and external. The internal part includes components that are directly integrated with the PID controller system and DC motor, while the external part includes supporting elements that serve to optimize the performance of the entire system. Figure 6-a shows the internal hardware implementation, while Figure 6-b displays the external hardware configuration.

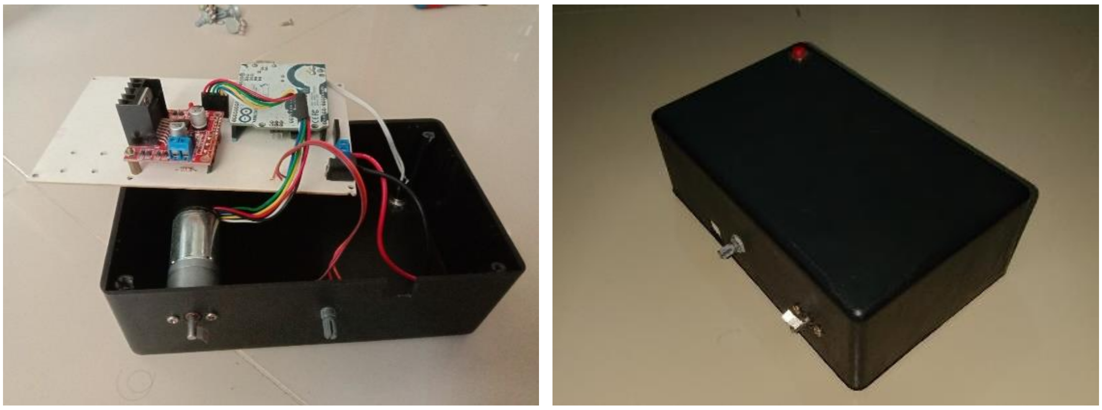

(a) (b)

Figure 6. (a) Internal and (b) External Hardware Configuration

3-2- Pulse Width Modulation (PWM) and Angular Sensor Experiments

In the PWM test that has been carried out, the results of the voltage value with the tested PWM value are obtained. This test is done by comparing the results of mathematical calculations using Equation 1 with direct testing. Table 2 displays the test results of the voltage value of each PWM.

Table 2. Voltage Experiments each PWM

PWM	Voltage Value (V)	Calculated Voltage Value (V)	Error (%)
50	2.17	2.353	8.433
75	3.31	3.529	6.616
100	4.36	4.706	7.936
125	5.53	5.882	6.365
150	6.62	7.059	6.631
175	7.75	8.235	6.258
200	8.82	9.412	6.712
225	10.08	10.588	5.040
250	11.14	11.765	5.610
Average error			**6.622**

Table 2 presents six sets of tested PWM values, namely 50, 75, 100, 125, 150, 175, 200, 225, and 250. Each PWM value has a voltage value that is measured directly on the DC motor. The results of these measurements are recorded in the “Voltage Value (V)” column in the table. As a comparison, a mathematical calculation using Equation (1) is performed, and the results are documented in the “Calculated Voltage Value (V)” column. The percentage error for each pair of measured and calculated voltage values was calculated in the error analysis. The percentage error is calculated using the formula in Equation 3.

$$Error\ (\%) = \left(\frac{Calculated\ value - Voltage\ value}{Voltage\ value}\right) \times 100\% \quad (3)$$

The results of the percentage error calculation for each PWM value are documented in the “Error (%)” column. The average error of the entire test is also calculated. Based on the table results, it can be seen that there is a difference between the directly measured voltage value and the mathematically calculated value for each PWM value. The average error of the entire test is 6.622%. The efficiency of the motor driver influences the average error value. Although there are variations, the test shows consistency in the error value, which can be a focus for improvement or performance enhancement in the PWM system.

The values of angular speed resulting from testing each PWM value are shown in Figure 7. The PWM was set to 50, 75, 100, 125, 150, 175, 200, 225, and 250. These experiments ensure that the angular speed sensor gives different RPM values with various PWM inputs. It can be observed that different PWM inputs give different angular speed values; a smaller value of PWM gives a smaller angular speed, and a bigger value of PWM gives a bigger angular speed. A multiplier constant factor of angular speed relative to the PWM values is different in each value of PWM. A small multiplier is found in PWM with high values, while a big multiplier is found in PWM with low values.

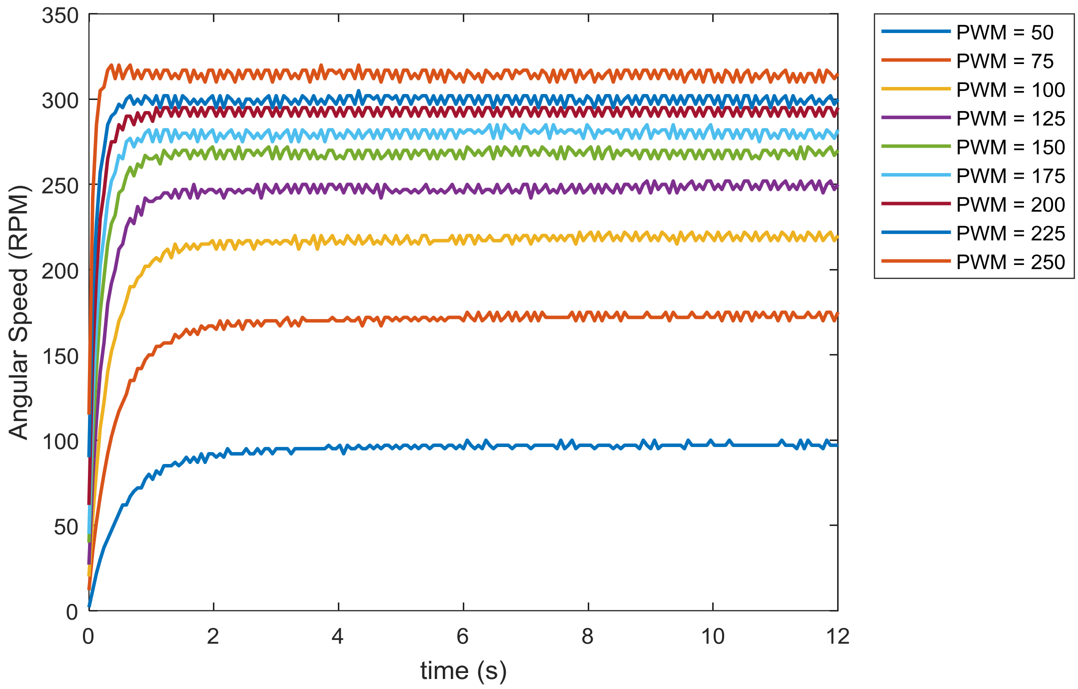

Figure 7. Angular Speed at each PWM

3-3- Proportional (P) Controller Experiments

Seven different proportional gain (Kp) parameter values were applied to analyze the influence of the P controller on the augmented system. Each Kp setting is used to control a DC motor with an angular speed setpoint of 100 RPM, which is set via a potentiometer attached to the system. This experiment aims to evaluate the system response to variations in the Kp parameter of proportional control. Seven different Kp values were applied to assess their effect on the stability and performance of the system in achieving the setpoint. The setpoint of 100 RPM provides a consistent basis for comparing the system response to changes in Kp. The use of a potentiometer as a setpoint control allows direct adjustment of the system, adding flexibility to the experiment. By varying Kp on the P controller, the optimal value that produces a stable and accurate system response to changes in angular velocity setpoint is expected to be found. This scientific approach provides a strong experimental basis for understanding and optimizing proportional control of DC motors to achieve specific angular speed targets. Figure 8 displays the P Controller test results, and Table 3 displays the system's responses.

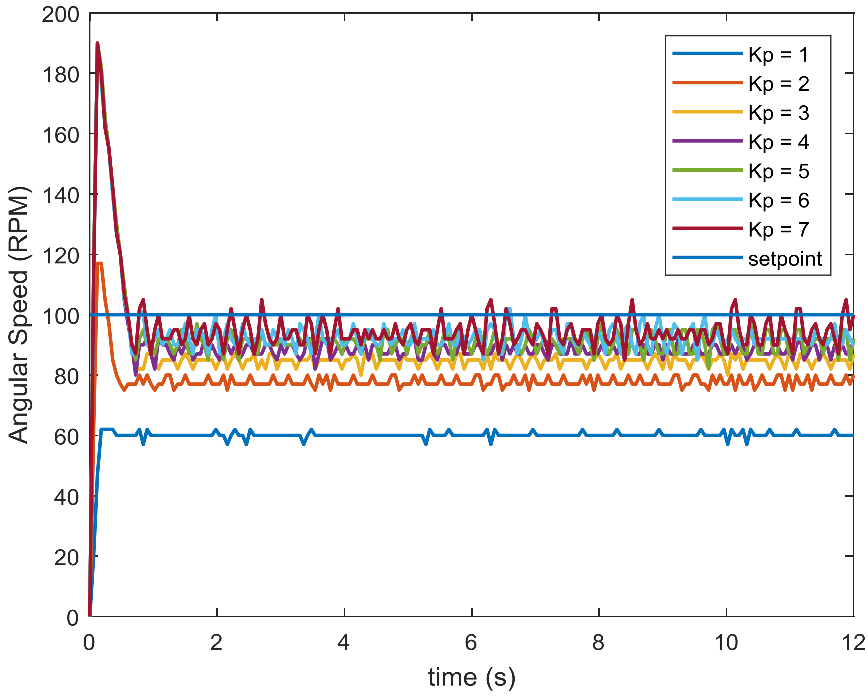

Figure 8. P Controller Experiments

Table 3. P Controller Analysis

Parameter	Rise time (s)	Settling time (s)	Overshoot (%)	Peak (RPM)	Peak time (s)
Kp=1	NaN	NaN	0	62	0.18
Kp=2	0.0631	11.9680	17	117	0.12
Kp=3	0.0363	11.9753	90	190	0.12
Kp=4	0.0384	11.9765	90	190	0.12
Kp=5	0.0384	11.9832	90	190	0.12
Kp=6	0.0385	11.9400	90	190	0.12
Kp=7	0.0428	11.9760	90	190	0.12

Table 3 presents the response analysis results of applying the P Controller on the DC motor with variation of proportional gain (Kp) parameter. The evaluation parameters include rise time, settling time, overshoot, Peak RPM, and Peak time, representing the characteristics of the system in response to changes in Kp. First, by setting Kp=1, the system was unable to reach a steady state, so rise time and settling time cannot be measured (NaN). Although the system's response had no overshoot, the Peak RPM achieved was 62 RPM with a Peak time of 0.18 seconds. Increasing the Kp value to 2 showed a significant increase in rise time (0.0631 seconds) and settling time (11.9680 seconds). An overshoot of 17% was found, with Peak RPM reaching 117 RPM at a peak time of 0.12 seconds. However, by increasing the Kp further to 3; 4; 5; 6; and 7, respectively, it can be observed that the rise time, settling time, and peak time experienced smaller changes, around 0.0384-0.0428 seconds, 11.9400-11.9832 seconds, and 0.12 seconds, respectively. Meanwhile, the overshoot value remained consistent at 90%, and the Peak RPM reached 190 RPM.

Generally, the analysis showed that increasing Kp resulted in a faster increase in reaching the setpoint (lower rise time) but also increased the overshoot rate. Although the settling time, overshoot, and peak time tended to be stable after using Kp=2, the significant increase in rise time may indicate that the optimal Kp value may lie in that range, resulting in a good balance between speed response and system stability.

3-4- Proportional Integral (PI) Controller Experiments

In the experiment, seven different proportional gain (Ki) parameters were combined with the same Kp parameter value, which was Kp = 1; the exact parameter value was chosen as the control parameter since no overshoot was found during the previous test. Each Ki setting is used to control a DC motor with an angular speed setpoint of 100 RPM, which is set through a potentiometer attached to the system. This experiment aims to evaluate the system response to variations in the Ki parameter of the proportional integral control. Seven different Ki values were applied to assess their effect on the stability and performance of the system in achieving the setpoint. The setpoint of 100 RPM provides a consistent basis for comparing the system response to changes in Ki. The use of a potentiometer as a setpoint control allows for direct adjustments to the system, adding flexibility to the experiment. By varying the Ki of the PI controller, the optimal value that produces a stable and accurate system response to changes in the angular velocity setpoint is expected to be found. This scientific approach provides a strong experimental basis for understanding and optimizing proportional control of DC motors to achieve specific angular speed targets. Figure 9 displays the PI Controller test results, and Table 4 displays the PI Controller test response analysis results.

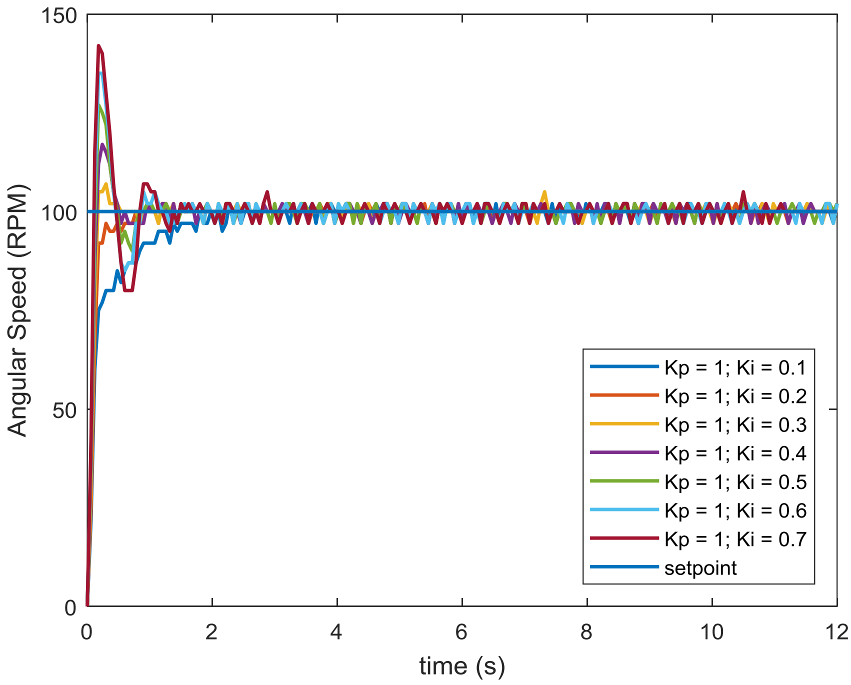

Figure 9. PI Controller Experiments

Table 4. PI Controller Analysis

Parameter	Rise time(s)	Settling time (s)	Overshoot (%)	Peak (RPM)	Peak time (s)
Kp=1, Ki=0.1	0.8127	11.952	2	102	2.28
Kp=1, Ki=0.2	0.1512	11.240	2	102	1.20
Kp=1, Ki=0.3	0.1278	11.952	7	107	0.30
Kp=1, Ki=0.4	0.1100	11.480	17	117	0.24
Kp=1, Ki=0.5	0.0986	11.660	27	127	0.18
Kp=1, Ki=0.6	0.0911	11.952	35	135	0.18
Kp=1, Ki=0.7	0.0852	10.940	42	142	0.18

Table 4 presents the results of the response analysis of the PI Controller on the DC motor with variations in the proportional gain (Kp) and integral gain (Ki) parameters. The evaluation parameters include rise time, settling time, overshoot, Peak RPM, and Peak time for each combination of Kp and Ki values. First, by setting Kp=1 combined with Ki=0.1, the augmented system responded in 0.8127 seconds of rise time and 11.952 seconds of settling time. A relatively small overshoot of 2% occurred, with the peak RPM reaching 102 RPM at a peak time of 2.28 seconds. By increasing Ki to 0.2, there was a significant improvement in the system response. The rise time decreased to 0.1512 seconds, and the settling time reached 11.240 seconds. Although the overshoot remained at 2%, the peak RPM occurred at a faster peak time of 1.20 seconds. Increasing Ki further to 0.3; 0.4; 0.5; 0.6; and 0.7 resulted in a consistent decrease in the rise time that can be observed, which reached its minimum at Ki=0.5 (0.0986 seconds). Settling time also decreased to 11.660 seconds at Ki=0.5. However, there was an increase in the overshoot rate, which reached a maximum of 35% at Ki=0.6. Although there was a decrease in overshoot when Ki=0.7 was applied, the rise time and settling time increased.

Overall, the analysis results showed that increasing Ki in the PI controller can reduce the rise time and settling time but was often followed by an increase in the overshoot. Therefore, when selecting Kp and Ki parameters in the PI Controller, the balance between response time and system stability level needs to be considered..

3-5- Proportional Integral Derivative (PID) Controller Experiments

The PID controller was tested by applying seven differential gain (Kd) parameter variations to achieve the best response to the DC motor. The angular speed setpoint of 100 RPM was set using a potentiometer attached to the system. The selection of the proportional gain (Kp) parameter value of 1 and integral gain (Ki) of 3 was based on previous testing results, where the configuration showed a low overshoot of 7% in reaching a peak time of less than 0.5 seconds. The settings of Kp=1 and Ki=3 were chosen to provide a basis for potential PID control configurations. The focus on Kd variation aims to find the optimum value to improve the system response to angular speed setpoint changes. The selection of Kd as the variable to be varied allows exploration of the influence of the differential control on the system's overall performance. Thus, this experiment was designed to understand and optimize the PID controller parameters to achieve a stable and accurate response to a DC motor with a specific setpoint. Figure 10 displays the PID Controller test results, and Table 5 displays the PID Controller test response analysis results.

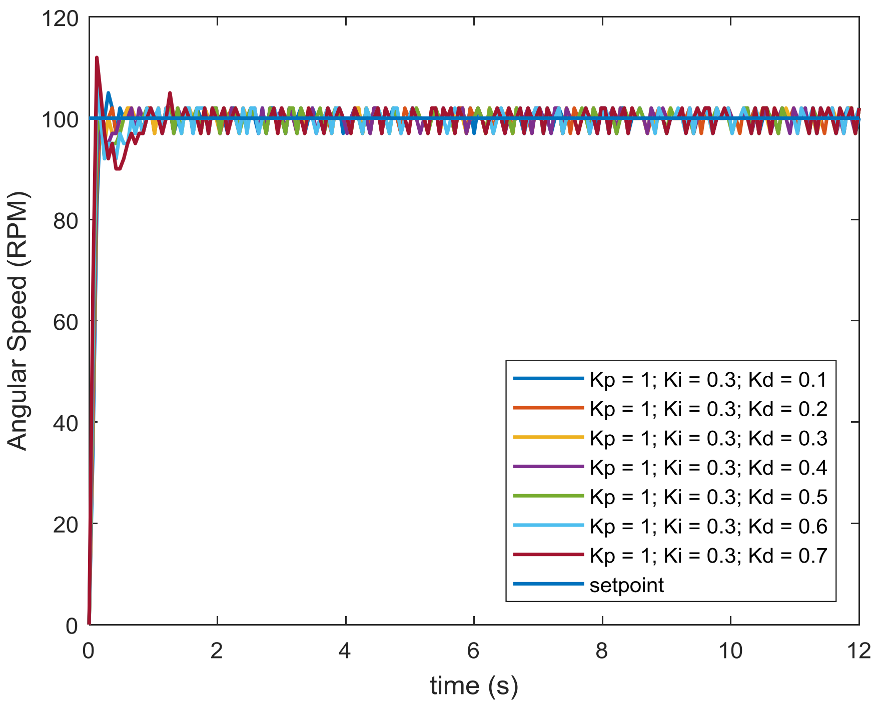

Figure 10. PID Controller Experiments

Table 5. PID Controller Analysis

Parameter	Rise time (s)	Settling time (s)	Overshoot (%)	Peak (RPM)	Peak time (s)
Kp=1, Ki=0.3, Kd=0.1	0.1269	11.960	5	105	0.30
Kp=1, Ki=0.3, Kd=0.2	0.1188	11.952	2	102	0.36
Kp=1, Ki=0.3, Kd=0.3	0.1033	11.952	2	102	0.60
Kp=1, Ki=0.3, Kd=0.4	0.1046	11.952	2	102	0.66
Kp=1, Ki=0.3, Kd=0.5	0.0991	11.952	2	102	0.90
Kp=1, Ki=0.3, Kd=0.6	0.0890	11.772	7	107	0.12
Kp=1, Ki=0.3, Kd=0.7	0.0817	11.952	12	112	0.12

Table 5 presents the results of the PID Controller response analysis on the DC motor with variations of combinations in the proportional gain (Kp), integral gain (Ki), and differential gain (Kd) parameters. The evaluation parameters include rise time, settling time, overshoot, peak RPM, and peak time for each combination of Kp, Ki and Kd values. In the configuration of Kp=1; Ki=0.3; with various values of Kd, it can be observed that increasing Kd significantly affects the system response. Increasing Kd from 0.1 to 0.5 resulted in a consistent decrease in rise time, with the lowest value achieved at Kd=0.6 (0.0890 seconds). Settling time also experienced a general decrease, reaching the lowest value at Kd=0.6 (11.772 seconds). Although the overshoot value remained low (2%) at all Kd variations, the change in Kd influenced the peak RPM and peak time values. An increase in Kd caused an increase in Peak RPM, with the highest value reached at Kd=0.6 (107 RPM). The peak time varied but remained relatively small within 0.12-0.90 seconds.

The best parameter recommendation can be made based on the trade-off between the rise time, settling time, and overshoot values. In this context, the PID Controller configuration with Kp=1; Ki=0.3; and Kd=0.6 showed good performance with low rise time, optimal settling time, and low overshoot (below 10%). Therefore, the best parameter recommendation is Kp=1; Ki=0.3; and Kd=0.6 to achieve the best response on a DC motor with a setpoint of 100 RPM. We then compared the experiment results with other results from previous studies. The performance comparison result is shown in Table 6. Based on the Table, the result of this research displayed the best rise time. The system's responses in the steady condition had stable oscillation due to the settling time of 11.952 seconds. Other studies' results did not have oscillation in their steady conditions.

Table 6. Comparison Result

Ref.	Parameter	Rise time (s)	Settling time (s)	Overshoot (%)
Najem et al. (2024) [65]	Kp=0.95, Ki=1.758, Kd=0.000127	0.520	0.644	0.81
Kurniasari & Ma'arif (2024) [66]	Kp=1, Ki=0.4, Kd=0.01	0.1751	1.2420	1.6287
Rahayu et al. (2022) [67]	Kp=0.8, Ki=0.877, Kd=0.629	1.5979	5.6667	2
Suseno & Ma'Arif (2021) [68]	Kp=3.75, Ki=1.3184, Kd=0.2051	2.7872	13.5	2
Present Study	Kp=1, Ki=0.3, Kd=0.5	0.0991	11.952	2

4- Conclusion

This research presents the angular speed control of a DC Motor with a PID Controller using an Arduino microcontroller, encoder sensor and motor driver. Based on the experiments, the PID method was successfully applied to control a 25-GA370 type DC motor equipped with an encoder sensor using the Arduino Uno platform. The experimental results show that the PID parameters significantly affect the system response. Increasing proportional value affects the rise time system to be bigger. Increasing the integral value helps the system reduce the steady state error but makes the rise time bigger. Increasing the derivative value affects the rise time to be smaller. Optimal results were obtained with parameters of Kp=1, Ki=0.3 and Kd=0.6, resulting in a rise time of 0.0890 seconds, a settling time of 11.772, a peak time of 0.12 seconds and an overshoot of less than 10% (7%). This shows that using PID with suitable parameters can precisely control the DC motor. Future research about controlling the DC motor angular speed can be implemented with other controllers such as nonlinear [69], robust, and/or adaptive control. Other future research works are to apply optimization algorithms [70], such as metaheuristic algorithms, to the controller.

5- Declarations

5-1- Author Contributions

Conceptualization, A.M.; methodology, A.M.; software, I.N.; validation, A.M.; formal analysis, A.M.; investigation, I.N.; writing—original draft preparation, I.N.; writing—review and editing, F.F. and A.M.; supervision, A.M., H.M., and I.S. All authors have read and agreed to the published version of the manuscript.

5-2- Data Availability Statement

The data presented in this study are available in the article.

5-3- Funding and Acknowledgements

This work was supported by Indonesia Endowment Fund for Education (LPDP), Ministry of Finance of the Republic of Indonesia.

5-4- Institutional Review Board Statement

Not applicable.

5-5- Informed Consent Statement

Not applicable.

5-6- Conflicts of Interest

The authors declare that there is no conflict of interest regarding the publication of this manuscript. In addition, the ethical issues, including plagiarism, informed consent, misconduct, data fabrication and/or falsification, double publication and/or submission, and redundancies have been completely observed by the authors.

6- References

[1] Mohanraj, D., Aruldavid, R., Verma, R., Sathiyasekar, K., Barnawi, A. B., Chokkalingam, B., & Mihet-Popa, L. (2022). A Review of BLDC Motor: State of Art, Advanced Control Techniques, and Applications. IEEE Access, 10, 54833–54869. doi:10.1109/ACCESS.2022.3175011.

[2] Kuczmann, M. (2024). Review of DC Motor Modeling and Linear Control: Theory with Laboratory Tests. Electronics (Switzerland), 13(11), 2225. doi:10.3390/electronics13112225.

[3] Ylldlrlm, Ş., Bingol, M. S., & Savas, S. (2024). Tuning PID controller parameters of the DC motor with PSO algorithm. International Review of Applied Sciences and Engineering, 15(3), 281–286. doi:10.1556/1848.2023.00698.

[4] Natawangsa, H., Furizal, Ma'arif, A., & Salah, W. A. (2025). Solution Stirring Design Using Magnetic Stirrer on DC Motor with PLC-Based PID Method. Jurnal Ilmiah Teknik Elektro Komputer Dan Informatika (JITEKI), 11(1), 42–52. doi:10.26555/JITEKI.V11I1.26534.

[5] Turan, A. (2025). Improved PID Control Design for Electric Power Steering DC Motor. IEEE Access, 13, 6080–6088. doi:10.1109/ACCESS.2024.3524303.

[6] Zarkasi, A., Ubaya, H., Exaudi, K., & Duri, A. H. (2024). Implementation of Fisherface Algorithm for Eye and Mouth Recognition in Face-Tracking Mobile Robot. Jurnal Ilmiah Teknik Elektro Komputer Dan Informatika (JITEKI), 10(3), 556–565. doi:10.26555/jiteki.v10i3.29266.

[7] Khan, H., Khatoon, S., & Gaur, P. (2021). Comparison of various controller design for the speed control of DC motors used in two wheeled mobile robots. International Journal of Information Technology, 13(2), 713-720. doi:10.1007/s41870-020-00577-8.

[8] Hendriyanto, R. D., Puriyanto, R. D., Ma'arif, A., Vera, M. A. M., Nugroho, O. I. A., & Chivon, C. (2024). Control of Water Flow Rate in a Tank Using the Integral State Feedback Based on Arduino Uno. Control Systems and Optimization Letters, 2(3), 357–365. doi:10.59247/csol.v2i3.162.

[9] Molina-Santana, E., Iturralde Carrera, L. A., Álvarez-Alvarado, J. M., Aviles, M., & Rodríguez-Resendiz, J. (2025). Modeling and Control of a Permanent Magnet DC Motor: A Case Study for a Bidirectional Conveyor Belt's Application. Eng, 6(3), 42. doi:10.3390/eng6030042.

[10] Kudra, G., Balthazar, J. M., Tusset, A. M., Wasilewski, G., Stańczyk, B., & Awrejcewicz, J. (2022). Dynamics analysis and control of a pendulum driven by a DC motor via a slider-crank mechanism. Mechanical Systems and Signal Processing, 166, 108415. doi:10.1016/j.ymssp.2021.108415.

[11] Prasad, B., Kumar, R., & Singh, M. (2024). Analysis of DC motor for process control application using neural network predictive controller. Engineering Research Express, 6(2), 25004. doi:10.1088/2631-8695/ad3b66.

[12] Fazdi, M. F., & Hsueh, P. W. (2023). Parameters Identification of a Permanent Magnet DC Motor: A Review. Electronics (Switzerland), 12(12), 2559. doi:10.3390/electronics12122559.

[13] Jabari, M., Ekinci, S., Izci, D., Bajaj, M., & Zaitsev, I. (2024). Efficient DC motor speed control using a novel multi-stage FOPD(1 + PI) controller optimized by the Pelican optimization algorithm. Scientific Reports, 14(1), 22442. doi:10.1038/s41598-024-73409-5.

[14] Gopi, P., Srinivasan, S., & Krishnamoorthy, M. (2022). Disk margin based robust stability analysis of a DC motor drive. Engineering Science and Technology, an International Journal, 32, 101074. doi:10.1016/j.jestch.2021.10.006.

[15] Sonugür, G. (2025). Efficient speed control of DC motors: imitation learning with fuzzy logic expert systems. Automatika, 66(2), 306–320. doi:10.1080/00051144.2025.2480425.

[16] Shneen, S. W., Dakheel, H. S., & Abdullah, Z. B. (2023). Design and implementation of no load, constant and variable load for DC servo motor. Journal of Robotics and Control (JRC), 4(3), 323-329. doi:10.18196/jrc.v4i3.17387.

[17] Ekinci, S., Izci, D., & Hekimoğlu, B. (2021). Optimal FOPID Speed Control of DC Motor via Opposition-Based Hybrid Manta Ray Foraging Optimization and Simulated Annealing Algorithm. Arabian Journal for Science and Engineering, 46(2), 1395–1409. doi:10.1007/s13369-020-05050-z.

[18] Yang, X., Deng, W., & Yao, J. (2022). Neural network based output feedback control for DC motors with asymptotic stability. Mechanical Systems and Signal Processing, 164, 108288. doi:10.1016/j.ymssp.2021.108288.

[19] Zhi, Y., Weiqing, W., Jing, C., & Razmjooy, N. (2022). Interval linear quadratic regulator and its application for speed control of DC motor in the presence of uncertainties. ISA Transactions, 125, 252–259. doi:10.1016/j.isatra.2021.07.004.

[20] Almawla, A. M., Hussein, M. J., & Abdullah, A. T. (2024). A comparative study of DC motor speed control techniques using fuzzy, SMC and PID. Journal Européen des Systèmes Automatisés, 57(2), 397. doi:10.18280/jesa.570209.

[21] Suwarno, I., Finayani, Y., Rahim, R., Alhamid, J., & Al-Obaidi, A. R. (2022). Controllability and Observability Analysis of DC Motor System and a Design of FLC-Based Speed Control Algorithm. Journal of Robotics and Control (JRC), 3(2), 227–235. doi:10.18196/jrc.v3i2.10741.

[22] Manuel, N. L., İnanç, N., & Lüy, M. (2023). Control and performance analyses of a DC motor using optimized PIDs and fuzzy logic controller. Results in Control and Optimization, 13, 100306. doi:10.1016/j.rico.2023.100306.

[23] Eker, E., Kayri, M., Ekinci, S., & Izci, D. (2021). A New Fusion of ASO with SA Algorithm and Its Applications to MLP Training and DC Motor Speed Control. Arabian Journal for Science and Engineering, 46(4), 3889–3911. doi:10.1007/s13369-020-05228-5.

[24] Ekinci, S., Hekimoğlu, B., & Izci, D. (2021). Opposition based Henry gas solubility optimization as a novel algorithm for PID control of DC motor. Engineering Science and Technology, an International Journal, 24(2), 331–342. doi:10.1016/j.jestch.2020.08.011.

[25] Izci, D. (2021). Design and application of an optimally tuned PID controller for DC motor speed regulation via a novel hybrid Lévy flight distribution and Nelder–Mead algorithm. Transactions of the Institute of Measurement and Control, 43(14), 3195–3211. doi:10.1177/01423312211019633.

[26] Kamarudin, M. N., Rozali, S. M., Azam, S. N. M., Hairi, M. H., & Zakaria, M. I. (2025). Formulation of a Lyapunov-Based PID Controller for Level Control of a Coupled-Tank System. International Journal of Robotics and Control Systems, 5(3), 1758-1769. doi:10.31763/ijrcs.v5i3.1947.

[27] Al-Dabbagh, Z. A., & Shneen, S. W. (2025). Design of a PID Speed Controller for BLDC Motor with Cascaded Boost Converter for High-Efficiency Industrial Applications. International Journal of Robotics and Control Systems, 5(1), 22-46. doi:10.31763/ijrcs.v5i1.1601.

[28] Qi, Z., Shi, Q., & Zhang, H. (2020). Tuning of digital PID controllers using particle swarm optimization algorithm for a CAN-Based DC motor subject to stochastic delays. IEEE Transactions on Industrial Electronics, 67(7), 5637–5646. doi:10.1109/TIE.2019.2934030.

[29] Ekinci, S., Izci, D., & Yilmaz, M. (2023). Efficient Speed Control for DC Motors Using Novel Gazelle Simplex Optimizer. IEEE Access, 11, 105830–105842. doi:10.1109/ACCESS.2023.3319596.

[30] Supriadi, S., Wajiansyah, A., Zainuddin, M., & Putra, A. B. W. (2024). Optimization of Proportional Integral Derivative Controller for Omni Robot Wheel Drive by Using Integrator Wind-up Reduction Based on Arduino Nano. Journal of Robotics and Control (JRC), 5(6), 1690-1701. doi:10.18196/jrc.v5i6.21807.

[31] Baidya, D., Dhopte, S., & Bhattacharjee, M. (2023). Sensing System Assisted Novel PID Controller for Efficient Speed Control of DC Motors in Electric Vehicles. IEEE Sensors Letters, 7(1), 1-4. doi:10.1109/LSENS.2023.3234400.

[32] Abdullah, Z. B., Shneen, S. W., & Dakheel, H. S. (2023). Simulation Model of PID Controller for DC Servo Motor at Variable and Constant Speed by Using MATLAB. Journal of Robotics and Control (JRC), 4(1), 54–59. doi:10.18196/jrc.v4i1.15866.

[33] Ekinci, S., Izci, D., Almomani, M. H., Saleem, K., Zitar, R. A., Smerat, A., Snasel, V., Ezugwu, A. E., & Abualigah, L. (2025). Advanced control parameter optimization in DC motors and liquid level systems. Scientific Reports, 15(1), 1–16. doi:10.1038/s41598-025-85273-y.

[34] Abdelghany, M. A., Elnady, A. O., & Ibrahim, S. O. (2023). Optimum PID Controller with Fuzzy Self-Tuning for DC Servo Motor. Journal of Robotics and Control (JRC), 4(4), 500–508. doi:10.18196/jrc.v4i4.18676.

[35] Tufenkci, S., Baykant Alagoz, B., Kavuran, G., Yeroglu, C., Herencsar, N., & Mahata, S. (2023). A theoretical demonstration for reinforcement learning of PI control dynamics for optimal speed control of DC motors by using Twin Delay Deep Deterministic Policy Gradient Algorithm. Expert Systems with Applications, 213, 119192. doi:10.1016/j.eswa.2022.119192.

[36] Martins, O. O., Adekunle, A. A., Arowolo, M. O., Uguru-Okorie, D. C., & Bolaji, B. O. (2022). The effect of an evolutionary algorithm's rapid convergence on improving DC motor response using a PID controller. Scientific African, 17, 1327. doi:10.1016/j.sciaf.2022.e01327.

[37] Nethaji, G., & Kathirvelan, J. (2024). Performance comparison between PID and Fuzzy logic controllers for the hardware implementation of traditional high voltage DC-DC boost converter. Heliyon, 10(17), e36750. doi:10.1016/j.heliyon.2024.e36750.

[38] Cabré, T. P., Vela, A. S., Ribes, M. T., Blanc, J. M., Pablo, J. R., & Sancho, F. C. (2021). Didactic platform for DC motor speed and position control in Z-plane. ISA Transactions, 118, 116–132. doi:10.1016/j.isatra.2021.02.020.

[39] Thangavel, S., Mohanraj, D., Girijaprasanna, T., Raju, S., Dhanamjayulu, C., & Muyeen, S. M. (2023). A Comprehensive Review on Electric Vehicle: Battery Management System, Charging Station, Traction Motors. IEEE Access, 11, 20994–21019. doi:10.1109/ACCESS.2023.3250221.

[40] Migliazza, G., Buticchi, G., Carfagna, E., Lorenzani, E., Madonna, V., Giangrande, P., & Galea, M. (2021). DC Current Control for a Single-Stage Current Source Inverter in Motor Drive Application. IEEE Transactions on Power Electronics, 36(3), 3367–3376. doi:10.1109/TPEL.2020.3013301.

[41] Barkas, D. A., Ioannidis, G. C., Psomopoulos, C. S., Kaminaris, S. D., & Vokas, G. A. (2020). Brushed dc motor drives for industrial and automobile applications with emphasis on control techniques: A comprehensive review. Electronics (Switzerland), 9(6), 887. doi:10.3390/electronics9060887.

[42] Valencia, D. F., Tarvirdilu-Asl, R., Garcia, C., Rodriguez, J., & Emadi, A. (2021). Vision, Challenges, and Future Trends of Model Predictive Control in Switched Reluctance Motor Drives. IEEE Access, 9, 69926–69937. doi:10.1109/ACCESS.2021.3078366.

[43] Swaminathan, R., Cai, C. J., Yuan, S., & Ren, H. (2021). Multiphysics Simulation of Magnetically Actuated Robotic Origami Worms. IEEE Robotics and Automation Letters, 6(3), 4923–4930. doi:10.1109/LRA.2021.3068707.

[44] Liu, W., Wang, J., & Lipo, T. A. (2023). A Consequent Pole Single Rotor Single Stator Vernier Design to Effectively Improve Torque Density of an Industrial PM Drive. IEEE Transactions on Industrial Electronics, 70(1), 255–264. doi:10.1109/TIE.2022.3153806.

[45] Yan, S., Yang, Y., Hui, S. Y., & Blaabjerg, F. (2021). A Review on Direct Power Control of Pulsewidth Modulation Converters. IEEE Transactions on Power Electronics, 36(10), 11984–12007. doi:10.1109/TPEL.2021.3070548.

[46] Arehpanahi, M., & Entekhabi, A. M. (2022). A New Technique for Online Open Switch Fault Detection and Location in Single-phase Pulse Width Modulation Rectifier. International Journal of Engineering, Transactions B: Applications, 35(9), 1759–1764. doi:10.5829/ije.2022.35.09c.12.

[47] Puentes, K., Morales, L., Pozo-Espin, D. F., & Moya, V. (2024). Enhancing Control Systems with Neural Network-Based Intelligent Controllers. Emerging Science Journal, 8(4), 1243–1261. doi:10.28991/ESJ-2024-08-04-01.

[48] Szczepankowski, P., Poliakov, N., Vertegel, D., Szwarc, K. J., & Strzelecki, R. (2020). A New Concept of PWM Duty Cycle Computation Using the Barycentric Coordinates in a Three-Dimensional Voltage Vectors Arrangement. IEEE Access, 8, 8019–8031. doi:10.1109/ACCESS.2019.2963743.

[49] Von Hoegen, A., Gotz, G. T., Mason, N. A., Hartgenbusch, N., Kojima, T., & De Doncker, R. W. (2024). Precise Volt-Second Measuring Instrument for PWM Voltage-Source Inverters. IEEE Transactions on Instrumentation and Measurement, 73, 1–15. doi:10.1109/TIM.2024.3381660.

[50] Thanoon, M. A., Almaged, M., & Abdulla, A. I. (2025). Boost Converter Control Using Proportional-Integral-Derivative Controller Optimized by Whale Optimization Algorithm. International Journal of Robotics & Control Systems, 5(3), 1850-1865. doi:10.31763/ijrcs.v5i3.1912.

[51] Mien, T. L., & Tu, T. N. (2024). Design and Quality Evaluation of the Position and Attitude Control System for 6-DOF UAV Quadcopter Using Heuristic PID Tuning Methods. International Journal of Robotics and Control Systems, 4(4), 1712–1730. doi:10.31763/ijrcs.v4i4.1594.

[52] Al-Samarraie, S. A., & Gorial, I. I. (2024). Assessment of FLC, PID, Nonlinear PID, and SMC Controllers for Level Stabilization in Mechatronic Systems. Journal of Robotics and Control (JRC), 5(6), 1845–1861. doi:10.18196/jrc.v5i6.23639.

[53] Bhookya, J., Vijaya Kumar, M., Ravi Kumar, J., & Seshagiri Rao, A. (2022). Implementation of PID controller for liquid level system using mGWO and integration of IoT application. Journal of Industrial Information Integration, 28, 100368. doi:10.1016/j.jii.2022.100368.

[54] Keppler, M., Raschel, C., Wandinger, D., Stemmer, A., & Ott, C. (2022). Robust Stabilization of Elastic Joint Robots by ESP and PID Control: Theory and Experiments. IEEE Robotics and Automation Letters, 7(3), 8283–8290. doi:10.1109/LRA.2022.3187277.

[55] Baghli, F. Z., Lakhal, Y., & El Kadi, Y. A. (2023). The Efficiency of an Optimized PID Controller Based on Ant Colony Algorithm (ACO-PID) for the Position Control of a Multi-articulated System. Journal of Robotics and Control (JRC), 4(3), 289–298. doi:10.18196/jrc.v4i3.17709.

[56] Mohammed, I. K., & Khalaf, L. A. (2024). Design and Simulation of an Analog Robust Control for a Realistic Buck Converter Model. Journal of Robotics and Control (JRC), 5(5), 1336–1348. doi:10.18196/jrc.v5i5.22408.

[57] Borase, R. P., Maghade, D. K., Sondkar, S. Y., & Pawar, S. N. (2021). A review of PID control, tuning methods and applications. International Journal of Dynamics and Control, 9(2), 818–827. doi:10.1007/s40435-020-00665-4.

[58] Alshalalfah, A. L., Hamad, G. B., & Mohamed, O. A. (2021). Towards Safe and Robust Closed-Loop Artificial Pancreas Using Improved PID-Based Control Strategies. IEEE Transactions on Circuits and Systems I: Regular Papers, 68(8), 3147–3157. doi:10.1109/TCSI.2021.3058355.

[59] Zellouma, D., Bekakra, Y., & Benbouhenni, H. (2023). Field-oriented control based on parallel proportional–integral controllers of induction motor drive. Energy Reports, 9, 4846–4860. doi:10.1016/j.egyr.2023.04.008.

[60] Chotikunnan, P., Chotikunnan, R., Nirapai, A., Wongkamhang, A., Imura, P., & Sangworasil, M. (2023). Optimizing Membership Function Tuning for Fuzzy Control of Robotic Manipulators using PID-Driven Data Techniques. Journal of Robotics and Control (JRC), 4(2), 128–140. doi:10.18196/jrc.v4i2.18108.

[61] Euzebio, T. A. M., Silva, M. T. D., & Yamashita, A. S. (2021). Decentralized PID Controller Tuning Based on Nonlinear Optimization to Minimize the Disturbance Effects in Coupled Loops. IEEE Access, 9, 156857–156867. doi:10.1109/ACCESS.2021.3127795.

[62] Joseph, S. B., Dada, E. G., Abidemi, A., Oyewola, D. O., & Khammas, B. M. (2022). Metaheuristic algorithms for PID controller parameters tuning: review, approaches and open problems. Heliyon, 8(5), 9399. doi:10.1016/j.heliyon.2022.e09399.

[63] Putra, A. M., Maradona, H., & Rohmah, R. A. (2025). Comparison of Proportional Integral Derivative and Fuzzy Logic Controllers: A Literature Review on the Best Method for Controlling Direct Current Motor Speed. International Journal of Robotics and Control Systems, 5(1), 240–265. doi:10.31763/ijrcs.v5i1.1701.

[64] Baharuddin, A., & Mohd Basri, M. A. (2023). Self-Tuning PID Controller for Quadcopter using Fuzzy Logic. International Journal of Robotics and Control Systems, 3(4), 728–748. doi:10.31763/ijrcs.v3i4.1127.

[65] Najem, A., Moutabir, A., & Ouchatti, A. (2024). Simulation and Arduino Hardware Implementation of ACO, PSO, and FPA Optimization Algorithms for Speed Control of a DC Motor. International Journal of Robotics and Control Systems, 4(3), 1186–1206. doi:10.31763/ijrcs.v4i3.1483.

[66] Kurniasari, I. D., & Ma'arif, A. (2024). Implementing PID-Kalman Algorithm to Reduce Noise in DC Motor Rotational Speed Control. International Journal of Robotics and Control Systems, 4(2), 958–978. doi:10.31763/ijrcs.v4i2.1309.

[67] Rahayu, E. S., Ma'arif, A., & Cakan, A. (2022). Particle Swarm Optimization (PSO) Tuning of PID Control on DC Motor. International Journal of Robotics and Control Systems, 2(2), 435–447. doi:10.31763/ijrcs.v2i2.476.

[68] Suseno, E. W., & Ma'Arif, A. (2021). Tuning of PID Controller Parameters with Genetic Algorithm Method on DC Motor. International Journal of Robotics and Control Systems, 1(1), 41–53. doi:10.31763/ijrcs.v1i1.249.

[69] Zheng, X., Yu, X., Jiang, J., & Yang, X. (2024). Practical Finite-Time Command Filtered Backstepping With its Application to DC Motor Control Systems. IEEE Transactions on Industrial Electronics, 71(3), 2955–2964. doi:10.1109/TIE.2023.3269478.

[70] Kong, W., Zhang, H., Yang, X., Yao, Z., Wang, R., Yang, W., & Zhang, J. (2024). PID control algorithm based on multistrategy enhanced dung beetle optimizer and back propagation neural network for DC motor control. Scientific Reports, 14(1), 1–26. doi:10.1038/s41598-024-79653-z.